Hyperfine Interact (2010) 195:275–280
DOI 10.1007/s10751-009-0129-z

Synthesis and characterization of superparamagnetic iron oxide nanoparticles for biomedical applications

L. A. Cano · M. V. Cagnoli · S. J. Stewart · E. D. Cabanillas · E. L. Romero · S. G. Marchetti

Published online: 25 September 2009

Abstract Monodisperse iron oxide nanoparticles (NPs) of 4 nm were obtained through high-temperature solution phase reaction of iron (III) acetylacetonate with 1, 2-hexadecanediol in the presence of oleic acid and oleylamine. The as-synthesized iron oxide nanoparticles have been characterized by X-ray diffraction, transmission electron microscopy, Mössbauer spectroscopy and magnetic measurements. The species obtained were Fe_3O_4 and/or γ-Fe_2O_3. These NPs are superparamagnetic at room temperature and even though the reduced particle size they show a high saturation magnetization (MS $\approx$ 90 emu/g).

Keywords Magnetic nanoparticles · Drug delivery systems · Mössbauer spectroscopy · Medical applications · Magnetite

1 Introduction

The use of magnetic NPs in drug delivery offer exciting new opportunities, since it is feasible to produce, and specifically tailor their functional properties for these

L. A. Cano · M. V. Cagnoli · S. G. Marchetti (✉)
CINDECA, Facultad de Ciencias Exactas, UNLP, CCT, CONICET,
Calle 47 N° 257, 1900 La Plata, Argentina
e-mail: march@quimica.unlp.edu.ar

S. J. Stewart
IFLP, CAC–La Plata, CONICET, Departamento de Física,
Facultad de Ciencias Exactas, Universidad Nacional de La Plata,
49 y 115, 1900 La Plata, Argentina

E. D. Cabanillas
Departamento de Materiales, CNEA, Av. del Libertador 8250,
1429 Buenos Aires, Argentina

E. L. Romero
Departamento de Ciencia y Tecnología, Universidad Nacional de Quilmes,
Sáenz Peña 180, Bernal 1876, Buenos Aires, Argentina

applications. Thus, drug targeting to tumours would be desirable since anticancer agents demonstrate non-specific toxicities that significantly limit their therapeutic potentials [1]. In these applications, a drug is bound to a magnetic compound, introduced in the body, and then concentrated in the target area by means of an external magnetic field gradient. Then, the particles must release the drug by simple diffusion or through mechanisms requiring enzymatic activity or changes in physiological conditions such as pH, osmolality, or temperature; drug release can also be magnetically activated using a thermosensitive grafted polymeric system (drug–polymer–magnetic NPs composite) which can be triggered to release the loaded drug with an increase in temperature, induced by an external alternating current magnetic field.

The key parameters in the behavior of magnetic NPs designed for such purposes are related to: (1) surface chemistry, (2) size: magnetic core, hydrodynamic volume, size distribution, (3) magnetic properties: superparamagnetism and high saturation magnetization. Sufficiently reduced size of magnetic NPs is adequate to achieve superparamagnetic regime, which is in turn needed to avoid magnetic agglomeration once the magnetic field is removed. But small particle size implies a magnetic response of reduced strength (i.e., a saturation magnetization diminished), making it difficult to direct particles and keep them in the proximity of the target while withstanding the drag of blood flow. On the other hand, negligible remanence and coercivity inhibit agglomeration and the possible embolization of capillary vessels is avoided.

A great number of NPs of different compounds are currently investigated, but the magnetic iron oxide NPs are very attractive for biomedical applications due to their biocompatibility. For this reason the aim of the present work is to verify whether iron oxide magnetic NPs—synthesized following the recipe of Sun et al. [2], with certain modifications to obtain a particle size lower than these authors—are potentially suitable to be used as effective drug delivery system. The as-prepared magnetic NPs are characterized by means of X-ray diffraction (XRD), transmission electron microscopy (TEM), Mössbauer spectroscopy (MS) and magnetic measurements (MM).

2 Experimental

The iron oxide NPs were obtained by mixing iron (III) acetylacetonate (6 mmol), 1, 2-hexadecanediol (30 mmol), oleic acid (18 mmol), oleylamine (18 mmol), and phenyl ether (60 ml). The mixture was magnetically stirred under a flow of nitrogen. Then, it was heated to 473 K for 30 min and after, under a blanket of nitrogen, heated to reflux (518 K) for another 30 min.

It is worth mentioning that to obtain a lowest final particle size; the reflux temperature is 20 K lower than that proposed by Sun et al. [2]. The black–brown mixture was cooled to room temperature by removing the heat source. Under ambient conditions, ethanol (40 ml) was added to the mixture, and a black material was precipitated and separated via centrifugation. The black product was dissolved in hexane (30 ml) in the presence of oleic acid (∼0.15 ml) and oleylamine (∼0.15 ml). Centrifugation (6,000 rpm, 10 min) was applied to remove any undispersed residue. The product was then precipitated with ethanol, centrifuged (6,000 rpm, 10 min) to remove the solvent, and redispersed into hexane.

XRD patterns were obtained using a standard Philips PW-1710 diffractometer with a scintillation counter and an exit beam graphite monochromator. Cu Kα ($\lambda = 1.5406$ Å) radiation was used to obtain data in the $10° \leq 2\theta \leq 100°$ range.

TEM micrographs were taken using a Philips CM200 microscope working at 160 keV.

Mössbauer spectra were obtained in transmission geometry with a 512-channel constant acceleration spectrometer. A source of ^{57}Co in Rh matrix of nominally 50 mCi was used. Velocity calibration was performed against a 6 μm-thick α-Fe foil. All isomer shifts (δ) are referred to this standard. The temperature between 25 and 298 K was varied using a Displex DE-202 Closed Cycle Cryogenic System. The Mössbauer spectra were fitted using a commercial program named Recoil [3]. Lorentzian lines with equal linewidths were considered for each spectrum component.

The magnetic measurements were carried out using a Multipurpose Physical Magnetic System superconducting quantum interference device from Quantum Design. The magnetization *versus* magnetic field (*M–H*) loops were recorded at 2, 5 and 300 K up to a maximum magnetic field of 50 kOe.

3 Results and discussion

The XRD data (not shown here) display the pattern corresponding to a cubic spinel structure belonging to maghemite and/or magnetite. No evidence of hematite peaks was detected.

After subtracting the instrumental broadening we applied the integral breadths method [4] to separate size and strain broadening assuming that the first has a Cauchy profile and the second a Gaussian profile. Using a parabolic relationship between the convolution and both profiles proposed by Halder and Wagner [5] and a graphical method, we obtained an average particle size of 3 nm.

TEM micrographs showed a narrow distribution of spherical NPs. Figure 1 shows the corresponding histogram from where an average particle size of 4.0 ± 0.5 nm was estimated. Analysis of the ring diffraction patterns showed that the NPs present a cubic spinel structure, with lattice parameters corresponding to Fe_3O_4/γ-Fe_2O_3.

Strikingly, the room temperature Mössbauer spectrum does not show any absorption signal (Fig. 2). Coincidently, below the fusion temperature of oleic acid, i.e. $T_f = 281°$K, a central broad signal starts to appear. Thus, the absence of resonance above T_f can be due to the quasi-free motion of particles of small size coated by the surfactant that increases the nucleus recoil energy.

We observe that a magnetic signal is partially resolved at 25 K. Notwithstanding, the presence of a central signal and a curved background indicate that the blocking of particle moments is not complete, i.e., a fraction remains in a superparamagnetic regime. About 45% is in this regime, therefore, blocking temperature is very close to 25 K.

We fitted this spectrum assuming two relaxation states following the Blume and Tjon model [6]. We have considered six components, five of them to simulate the partially magnetically ordered magnetite sites [7] and the other one to account for the central signal. The hyperfine parameters are shown in Table 1. Comparing these parameters with previous reported data [7, 8] for magnetite bulk we assign the B_i

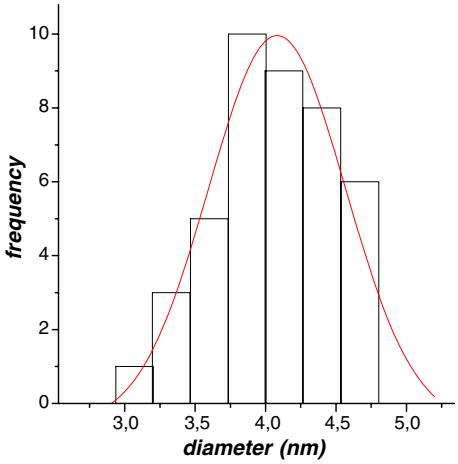

Fig. 1 Particle size histogram from TEM observations

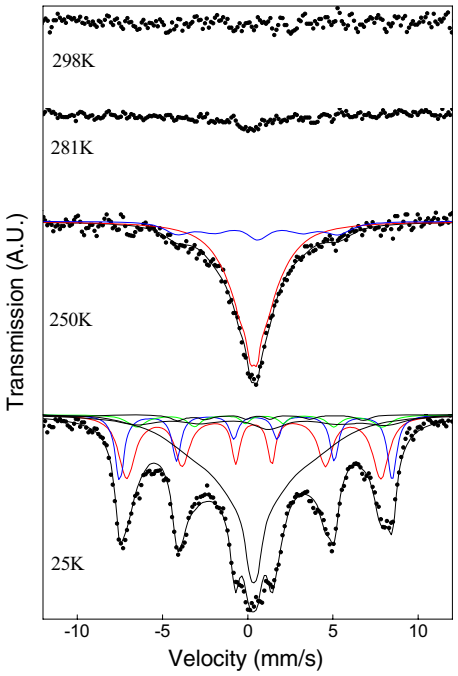

Fig. 2 Mössbauer spectra of magnetic NPs at different temperatures

components to Fe_3O_4. Note that hyperfine magnetic field of all sites are diminished in comparison with the bulk values. This effect could be attributed to the collective magnetic excitations produced by the small particle sizes [9]. The A component can not be assigned to any determined species but considering that their isomer shift is typical of Fe^{3+} it could belong to Fe_3O_4 and/or γ-Fe_2O_3.

The *M–H* loops are shown in Fig. 3. We observe that the curves are reversible down to T = 5 K, where we observe a very low coercive field of $H_C = 2$ Oe (see inset Fig. 1). Decreasing the temperature to 2 K, a hysteretic behavior is observed

Table 1 Hyperfine parameters at 25 K

Species	Sites	H (kOe)	δ (mm/s)	2ε (mm/s)	%
Fe_3O_4 and γ-Fe_2O_3	A	470 ± 4	0.36 ± 0.03	0.001 ± 0.005	25 ± 2
Fe_3O_4	B_1	508 ± 2	0.46 ± 0.02	0.03 ± 0.04	14 ± 2
	B_2	473 ± 14	0.83[a]	−0.27[a]	5 ± 2
	B_3	466[a]	1.03[a]	−0.41[a]	9 ± 4
	B_4	343 ± 24	0.96[a]	0.7 ± 0.5	2 ± 1
Relaxing Fe^{3+}	–	300[a]	0.35 ± 0.04	0[a]	45 ± 2

H hyperfine magnetic field, *δ* isomer shift referred to α-Fe at 298 K, *2ε* quadrupole shift
[a]Parameter held fixed while fitting

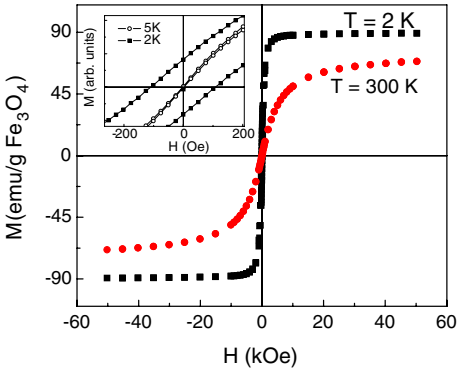

Fig. 3 M–H curves taken at 2 and 300 K. *Inset*: low field region of M vs. H loops taken at 2 and 5 K

with $H_C = 105$ Oe. The M_R/M_S ratio is ≈0.14, which is far from the $M_R/M_S = 0.5$ value predicted for independent NPs with uniaxial anisotropy [10]. Considering the area of the 2K-hysteresis loop we estimated an effective anisotropy constant $K_{\text{eff}} \approx 1.5 \times 10^5$ erg/cm^3, which is within the order of magnitude of the bulk value [11]. Therefore, the surface anisotropy constant could be considered negligible. A saturation magnetization $M_S = 89$ emu/g at T = 2 K was estimated assuming an *M vs. H* dependence of type $M = M_S(1\text{-}\alpha/H)$ at high magnetic fields, where α is a fitting parameter. This M_S, which is similar to that reported for bulk Fe_3O_4 (92 emu/g) [11] reflects the spin disorder absence at NPs surface even though the small particle sizes.

Generally, ferrimagnetic NPs present reduced *Ms* values when compared with their bulk counterparts due to the spin disorder at the surface layer. For instance, nanosized Fe_3O_4 can show a reduction of 80–90% on its M_S value [12, 13]. On the other hand, when these Fe_3O_4 NPs are coated with surfactants, the chemical environment of the coating may also influence on the magnetic properties [11, 14]. The present results are in concordance with that obtained by Guardia et al. [11], confirming that the O^{2-} of the oleic acid molecules bonded covalently to the nanoparticles are able to reduce the surface spin disorder and thus the surface contribution to the anisotropy [11] Considering that these NPs are superparamagnetic at room temperature with a high saturation magnetization, they would have potential applications in biomedicine.

4 Conclusions

We were able to synthesized monodisperse magnetic iron oxide NPs through the reaction of metal acetylacetonate and 1,2-hexadecanediol. Through different characterization techniques we determined a particle diameter of about 4 nm. The NPs composition is a mixture of both ferrimagnetic iron oxides: Fe_3O_4 and γ-Fe_2O_3, determined by Mössbauer spectroscopy. The magnetic properties of these NPs are very similar to that of the bulk system, perhaps due to the oleic coating effect. The hydrophobic NPs could be transformed into hydrophilic ones by mixing with bipolar surfactants, allowing preparation of aqueous NPs dispersions. These iron oxide NPs and their aqueous dispersions could have a great potential in biomedical applications.

Acknowledgements The authors acknowledge support of this work by Consejo Nacional de Investigaciones Científicas y Técnicas (PIP 6524), ANPCyT (PICT 38337) and Universidad Nacional de La Plata (X438), Argentina.

References

1. Jain, T.K., Morales, M.A., Sahoo, S.K., Leslie-Pelecky, D.L., Labhasetwar, V.: Mol. Pharm. **2**(3), 194 (2005)
2. Sun, S., Zeng, H., Robinson, D.B., Raoux, S., Rice, P.M., Wang, S.X., Li, G.: J. Am. Chem. Soc. **126**, 273 (2004)
3. Lagarec, K., Rancourt, D.G.: Mossbauer Spectral Analysis Software, Version 1.0. Department of Physics, University of Ottawa (1998)
4. Klug, H.P., Alexander, L.E.: X-ray Diffraction Procedures. Wiley, New York (1974)
5. Halder, N.C., Wagner, C.N.J.: Acta Crystallogr. **20**, 312 (1966)
6. Blume, M., Tjon, J.A.: Phys. Rev. **165**, 446 (1968)
7. Berry, F.J., Skinner, S., Thomas, M.F.: J. Phys.: Condens. Matter **10**, 215 (1998)
8. Vandenberghe, R.E., De Grave, E.: In: Long, G.J., Grandjean, F. (eds.) Mössbauer Spectroscopy Applied to Inorganic Chemistry, vol. 3, pp. 59. Plenum, New York (1989)
9. Mørup, S., Topsøe, H.: Appl. Phys. **11**, 63 (1976)
10. Stoner, E.C., Wohlfarth, E.P.: Phil. Tran. Roy. Soc. Lond., A **240**, 599 (1948)
11. Guardia, P., Batlle-Brugal, B., Roca, A.G., Iglesis, O., Morales, M.P., Serna, C.J., Labarta, A., Batle, X.: J. Magn. Magn. Mater. **316**, e756–e759 (2007)
12. Fellenz, N.A., Marchetti, S.G., Bengoa, J.F., Mercader, R.C., Stewart, S.J.: J. Magn. Magn. Mat. **306**, 30 (2006)
13. Kumar, R.V., Koltypin, Y., Cohen, Y.S., Cohen, Y., Aurbach, D., Palchik, O., Felner, I., Gedanken, A.: J. Mater. Chem. **10**, 1125 (2000)
14. Hou, Y., Yua, J., Gao, S.: J. Mater. Chem. **13**, 1983 (2003)